PKS 1018−42: A Powerful Kinetically Dominated Quasar

Brian Punsly

4014 Emerald Street No.116, Torrance CA, USA 90503 and International Center for Relativistic Astrophysics, I.C.R.A.,University of Rome La Sapienza, I-00185 Roma, Italy

brian.m.punsly@L-3com.com or brian.punsly@gte.net

and

Steven Tingay

Centre for Astrophysics and Supercomputing, Swinburne University of Technology, P.O. Box 218, Hawthorn, Vic 3122, Australia

stingay@astro.swin.edu.au

ABSTRACT

We have identified PKS 1018-42 as a radio galaxy with extraordinarily powerful jets, over twice as powerful as any 3CR source of equal or lesser redshift except for one (3C196). It is perhaps the most intrinsically powerful extragalactic radio source in the, still poorly explored, Southern Hemisphere. PKS 1018-42 belongs to the class of FR II objects that are kinetically dominated, the jet kinetic luminosity, $Q \sim 6.5 \times 10^{46}$ergs/s (calculated at 151 MHz), is 3.4 times larger than the total thermal luminosity (IR to X-ray) of the accretion flow, $L_{bol} \sim 1.9 \times 10^{46}$ergs/s. It is the fourth most kinetically dominated quasar that we could verify from existing radio data. From a review of the literature, we find that kinetically dominated sources such as PKS 1018-42 are rare, and list the 5 most kinetically dominated sources found from our review. Our results for PKS 1018-42 are based on new observations from the Australia Telescope Compact Array.

Subject headings: quasars: general — quasars: individual (PKS 1018−42) — galaxies: jets — galaxies: active — accretion disks — black holes

1. Introduction

The southern sky below a declination of -40° is still not well explored in the radio band compared to the northern sky and many of the intrinsically most powerful radio sources might not have ever been imaged in detail at radio wavelengths. Suspecting this to be the case, we began to search for evidence of the most powerful Southern Hemisphere radio sources from archival spectral information. Two sources stood out: PKS 0743−67 (reported in Punsly and Tingay (2005)); and PKS 1018−42.

In this Letter, we present the first deep radio observations of PKS 1018−42, a quasar at $z = 1.28$ (Hewitt & Burbidge 1993) with a 5 GHz flux density over 1.2 Jy (Gregory et al. 1994). The steep radio spectrum of PKS 1018−42 over a frequency range of 80 MHz (Slee 1995) to 31.4 GHz (Geldzahler & Witzel 1981) suggests that the source is dominated by optically thin radio lobe emission rather than Doppler-boosted core emission. Due to its southerly declination, there are no previously published deep radio maps of this extremely powerful object, however Ulvestad et al (1981) obtained VLA observations giving an indication of some source structure, but were not sufficient to reveal the detailed source morphology. Basic structural information from the VLA observations was limited only to the 20 cm waveband.

We have used Australia Telescope Compact Array (ATCA) observations to separate the core and lobe emission between 2.5 and 8.6 GHz, in order to caclulate the time-averaged kinetic luminosity of the jets, $Q \approx 6.5 \times 10^{46}$ergs/s, making PKS 1018−42 one of the most kinetically dominated quasars known.

In this paper we adopt the following cosmological parameters: H_0=70 km/s/Mpc, $\Omega_\Lambda = 0.7$ and $\Omega_m = 0.3$. We use the radio spectral index, α, as $S \propto \nu^{-\alpha}$.

2. The Radio Observations

The Australia Telescope Compact Array (ATCA) was used to obtain observations of PKS 1018−42 on December 16, 2001, in a series of 20 minute "cuts″ over a 12 hour period. For half of the cuts the ATCA was configured to observe at frequencies of 1384 and 2496 MHz (1.4 and 2.5 GHz) and at 4800 and 8640 MHz (4.8 and 8.6 GHz) for the other half. The observations took place while the array was in a 6 km baseline configuration, allowing maximum angular resolution. At all frequencies the bandwidth was 128 MHz in each of two crossed linear polarisations.

Standard data reduction and imaging techniques were used to produce images from the

data (Sault et al. 1995). Stokes I, Q, and U images were produced from the 2.5, 4.8, and 8.6 GHz data. It was found that the 1.4 GHz data proved of insufficient angular resolution to be useful. Figure 1 shows the resulting image of PKS 1018−42 at 4.8 GHz. A core is centrally located between two powerful lobes. Estimates of component sizes and positions were made by model-fitting the u-v data with point sources, circular Gaussian, and elliptical Gaussian components in the DIFMAP package (Shephard et al. 1994) and are summarized in Table 1.

We are confident that we have recovered the full flux density of the source at each frequency since at 8.6 GHz, our highest frequency and therefore highest angular resolution, our total measured flux density of 0.63 Jy matches the independently determined single dish flux density at this frequency (Wright et al. 1991). We note that the 8.6 GHz image implies an axial length of $14.9''$. In our adopted cosmology, this corresponds to an axial length of $D = 140$kpc.

3. Estimating the Jet Kinetic Luminosity

We estimate the jet kinetic luminosity from the isotropic extended emission, applying a method that allows one to convert 151 MHz flux densities, F_{151} (measured in Jy), into estimates of kinetic luminosity, Q (measured in ergs/s), following Willott et al. (1999) and Blundell and Rawlings (2000), by means of the formula derived in Punsly (2005):

$$Q \approx 1.1 \times 10^{45} \left[(1+z)^{1+\alpha} Z^2 F_{151}\right]^{\frac{6}{7}} \text{ergs/sec} \ , \tag{3-1}$$

$$Z \equiv 3.31 - (3.65) \times \left(\left[(1+z)^4 - 0.203(1+z)^3 + 0.749(1+z)^2 + 0.444(1+z) + 0.205\right]^{-0.125} \right) \ , \tag{3-2}$$

where F_{151} is the total optically thin flux density from the lobes (i.e., no contribution from Doppler boosted jets or radio cores). The formula is most accurate for large classical double radio sources which is the case for PKS 1018−42 (Willott et al. 1999).

A measurement of the lobe flux at low frequency is critical to the successful implementation of (3.1). Our estimate of the spectral index between 2.5 and 8.6 GHz for the northern lobe is $\alpha = 1.23$ and for the southern lobe is $\alpha = 1.03$. We estimate the core spectral index between 2.5 and 8.6 GHz as $\alpha = 1.14$. We cannot separate the core and lobes at 1.4 GHz due to poor angular resolution at this frequency. However, extrapolating the lobe spectra to 1.4 GHz and subtracting the lobe fluxes at this frequency gives us an estimate of the core flux density of 0.016 Jy. The core spectrum therefore appears to flatten to $\alpha = 0.49$ near 1 GHz. This being the case, the core appearing to turn over below 1 GHz, the core contribution to the total flux at 151 MHz will be negligible.

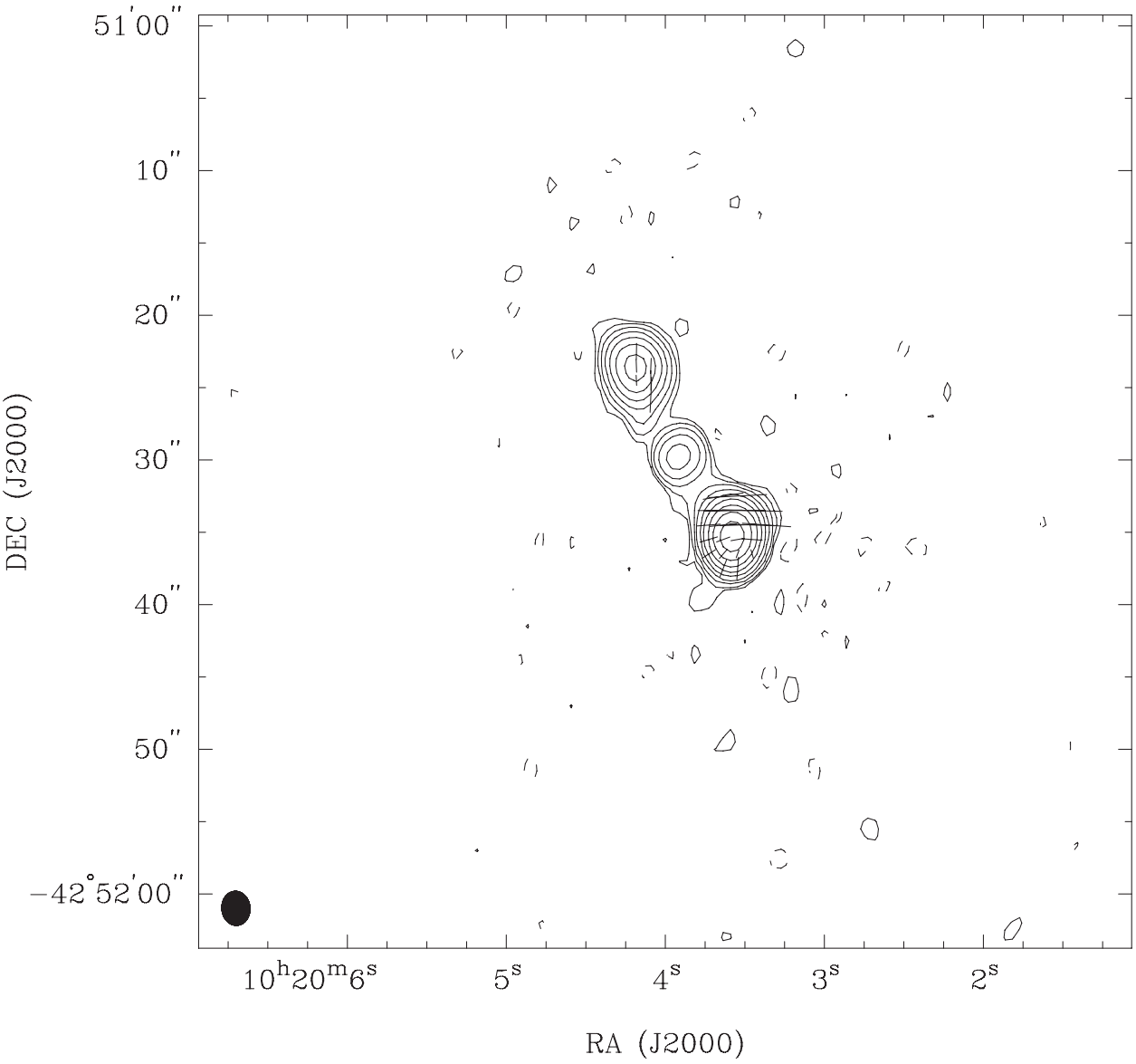

Fig. 1.— PKS 1018−42 at 4.8 GHz. The peak intensity in the image is 0.77 Jy/beam. The beam-size is 1.9″×2.3″at a position angle of 5.1°. Contour levels for the Stokes I emission are 0.0077 Jy/beam × (-0.25, 0.25, 0.5, 1, 2, 4, 8, 16, 32, 64). The peak fractional polarization is 18.5%. The vector lengths represent 4.4% fractional polarization per arcsecond.

Table 1: ATCA radio data for core and lobes of PKS 1018−42

Frequency MHz	Beam arcsec	Component	Flux Jy	FWHM arcsec	Notes
1384	7.4 × 5.7	North	1.07	3.4 × 1.5	
		Core	na	na	a
		South	3.16	1.9 × 1.3	
		Total	4.23		
2496	4.2 × 3.5	North	0.51	1.7 × 1.4	
		Core	0.12	5.7 × 1.3	b
		South	1.77	1.2 × 0.7	
		Total	2.40		
4800	2.3 × 1.9	North	0.24	1.5 × 1.1	
		Core	0.06	1.9 × 0.0	c
		South	0.96	1.3 × 0.7	
		Total	1.26		
8640	1.3 × 1.1	North	0.11	1.4 × 1.2	
		Core	0.03	0.5 × 0.0	
		South	0.49	na	d
		Total	0.63		

[a]Core not detected/resolved at 1384 MHz.

[b]Core detected but appears highly extended in direction of lobes. Probably lobe emission contaminating estimate of core flux and size.

[c]Core unresolved in direction perpendicular to the lobe direction.

[d]South lobe resolved into 4 sub components, between 0.01 and 0.20 Jy in flux and 0.5 and 1.0 arcseconds in size. Flux given is sum of subcomponent fluxes.

Extrapolating the lobe flux densities using the 2.5 to 8.6 GHz spectral indices yields flux densities of 16 Jy and 45 Jy at 408 MHz and 160 MHz, respectively. However, the 408 MHz and 160 MHz flux densities have been previously measured as 12.72 Jy, Large et al. (1981), and 25.5 Jy, Slee (1995), respectively. Thus, the lobe spectrum appears to flatten slightly at frequencies below 1 GHz. Using a spectral index derived from the measurements at 408 MHz and 160 MHz, and extrapolating to 151 MHz, yields $F_{151} = 26.4$, which can be used in (3.1) to give $Q \approx 6.5 \times 10^{46}$ergs/s. Alternatively, we can use our new 4.8 GHz flux from Table 1 with equation (3.9) of Punsly (2005), adapted to 4.8 GHz flux densities, F_{4800},

$$Q \approx 1.81 \times 10^{46}(1+z)^{1+\alpha} Z^2 F_{4800}\,\mathrm{ergs/sec}\ , \quad \alpha \approx 1\ . \tag{3-3}$$

to obtain a slightly larger estimate, $Q \approx 9.5 \times 10^{46}$ergs/s.

4. Kinetic Dominance of the Source

In this section we estimate R, the ratio of the kinetic luminosity, Q, to the total bolometric luminosity of the accretion flow, L_{bol}. Recall that L_{bol} is the bolometric luminosity of the thermal emission from the accretion flow, including any radiation in broad emission lines from photo-ionized gas or as IR reprocessed by molecular gas. In order to estimate L_{bol}, we construct a composite spectral energy distribution (SED) of a quasar accretion flow (Punsly and Tingay 2005). In order to separate the accretion flow thermal luminosity from IR and optical contamination from the jet, an SED for radio quiet quasars (normalized to $M_V = -25$) was chosen since this represents pure accretion luminosity. A piecewise collection of power laws in table 2 is used to approximate the individual bands in the SED. The first two columns are the start and stop frequencies for the each local power law. The third and fourth columns are the corresponding values of νF_ν. One can compute the L_{bol} of the accretion flow from the composite SED. In addition to the continuum, the composite spectrum of Zheng et al. (1997) indicates that $\approx 25\%$ of the total optical/UV quasar luminosity is reprocessed in the broad line region. Combining this with the continuum luminosity yields $L_{bol} = 1.35 \times 10^{46}$ergs/sec. Now if one assumes that the shape of the SED is unchanged with the magnitude of L_{bol} then Table 2 is particularly useful, since it allows the knowledge of IR, UV or X-ray flux to estimate L_{bol}. Namely, $L_{bol}/1.35 \times 10^{46}$ergs/sec scales with the value of the measured νF_ν divided by the value of νF_ν in the composite of Table 2 at the selected frequency of observation. With this assumption, the UV continuum flux density at the rest frame frequency of 1.37×10^{15}Hz in the spectrum of PKS 1018−42 in Stickel et al. (1994) applied to the composite in Table 2 yields $L_{bol} = 1.9 \times 10^{46}$ergs/s. Thus, $R = 3.4$ for the 151 MHz estimate of Q and $R = 5$ for the 4.8 GHz estimate of Q.

It is interesting to ask how rare it is to find a kinetically dominated quasar, $R > 1$. The

natural place to find $R > 1$ sources is to look at the highest redshift sources in a low radio frequency selected survey. To estimate R in quasars, one can use primarily UV emission and also reprocessed IR dust emission to estimate L_{bol} from Table 2 as a check for obscuration of the accretion disk. For FR II narrow line radio galaxies (hidden quasars), one can only use the reprocessed IR dust emission that peaks around $100\mu m$. In addition, a high resolution radio map is required to isolate the optically thin radio flux density that is required in (3.1).

To determine the rate of occurrence of kinetically dominated quasars, the UV data from Veron-Cetty and Veron (2001) were cross-correlated with archival VLA and MERLIN radio maps, in order to single out possible large R quasar candidates. The actual spectra (referenced in column 7 of table 3) of sources that looked promising were subsequently studied explicitly in order to compute L_{bol}. Similarly, submm data for high redshift, $z > 3.0$, sources (redshifted dust emission) in Archibald et al. (2001) and IR data for $z < 1.5$ sources from Meisenheimer et al. (2001) and Haas et al. (2004) were used to estimate L_{bol} for obscured quasars with powerful radio emission. An exhaustive search of the literature revealed very few sources with R larger than that of PKS 1018−42. We found deep radio observations of > 800 radio loud quasars primarily in the references Akujor et al (1991); Akujor and Garrington (1995); Antonucci and Ulvestad (1985); Bogers et al (1994); Hintzen et al (1983); Hutchings et al (1988); Liu et al (1992); Lonsdale et al (1993); Mantovani et al (1992); Murphy et al (1993); Neff et al (1989); Neff and Hutchings (1990); Punsly (1995); Reid et al (1999) with M_V tabulated in Veron-Cetty and Veron (2001). Additionally, there were another ~ 100 powerful FRII radio galaxies with IR data in Archibald et al. (2001); Meisenheimer et al. (2001); Haas et al. (2004) and deep radio observations. The large R sources are tabulated in Table 3. The first two columns are the source and its redshift, followed by Q and R computed with equation (3.1). The fifth column is the frequency in which a rest frame flux density was used to estimate L_{bol} from Table 2. The sixth column is the UV spectral index, when it was available. In spite of this search, two of the four highest R sources in Table 3, 3C 82 and PKS 1018−42 had no previously published radio maps and were found by looking for high redshift sources in Veron-Cetty and Veron (1991) with the largest low frequency flux densities and steep spectral indices. These were the most promising candidates out of the 6225 quasars. This initiated followup observations reported here and in Semenov et al. (2004).

The two estimates for both 3C 82 (the highest redshift 3C quasar known) and 3C 9 (the highest redshift 3CR quasar) in the IR and UV are in close agreement, verifying the validity of the composite in Table 2. Both 3C 405 and 3C 190 were added to the list of the five largest R sources for comparison purposes. 3C 405 (Cygnus A) is the best studied example of a very high Q radio galaxy and the close agreement between the X-ray and IR estimates for 3C 405

are also affirmation of the application of Table 2. Note the difference in the estimates for 3C 190. The IR and the continuum UV estimate at 1.34×10^{15}Hz disagree tremendously. This is because 3C 190 is an obscured quasar with a red spectrum, indicated by the steep UV spectral index of 3. Thus, a third estimate for 3C 190 is given, $L_{bol} = 1.07 \times 10^{15}$Hz, from the MgII broad emission line. According to Wang et al. (2004), $L_{bol} \approx 165 L_{MgII}$, where L_{MgII} is the line luminosity. This 3C 190 line estimate agrees with the IR estimate, consistent with an attenuated line of sight toward the accretion disk but not towards the low ionization broad line region. The main reason for including 3C 190 is the rather steep UV spectral index of PKS 1018−42. This might raise some concerns about a heavily obscured accretion flow that is skewing the estimate of R. We note that the MgII line estimator agrees with the UV continuum estimate for PKS 1018-42. Even though this is strongly supportive of the UV estimate of R, a space based IR measurement would be definitive.

5. Conclusion

In this Letter, we have investigated radio images of a very powerful quasar PKS 1018−42 that is not well known due to its southerly declination. However, PKS 1018-42 is extraordinarily powerful with jets over twice as powerful as any 3CR source of equal or lesser redshift except for one (3C196) and is certainly worthy of more detailed study. We found that it is kinetically dominated with $R \sim 3 - 5$. It is the fourth most kinetically dominated quasar that we could verify from existing radio maps.

We showed in Table 3 that kinetic dominance is a particularly rare circumstance for quasars. This is consistent with the study of 7C sources in Willott et al. (1999) that was based on estimating L_{bol} from OII narrow line emission. The OII narrow lines are very distant from the central quasar and it is not clear how much jet propagation excites narrow line emission (see Veilleux and Bland-Hawthorn (1997) for one of many examples of narrow line emission that is stimulated by jet propagation). Using the UV luminosity from the central quasar directly as we have done is far more reliable, especially when verified independently with IR and broad line data as was done above. Thus, our results are consistent with Willott et al. (1999), but they are found from an independent and perhaps more scientifically justified method. However, Table 3 is incomplete because the most likely large R candidates are high redshift 3C narrow line galaxies and the current $450\mu m$ sensitivity required for these estimates is not available, just loose bounds on the flux density (Archibald et al. 2001). Even if there are some kinetically dominated high z radio galaxies, this should not change the conclusion drawn from Table 3 that large values of R, such as for PKS 1018−42, are unusual for quasars.

The rarity of large R sources follows from the steep luminosity distributions for FR II quasars, 2×10^{45}ergs/s $< L_{bol} < 3 \times 10^{48}$ergs/s and 10^{44}ergs/s $< Q < 3 \times 10^{47}$ergs/s (Veron-Cetty and Veron 2001; Punsly 2001). A value of $R = 10$ requires $Q > 2 \times 10^{46}$ergs/s which is already at the high end of the steep kinetic luminosity distribution and these sources are rare. Yet, the complete absence of $R \sim 30$ sources still seems unexpected because Q is a measure of the long term activity of the radio source over $\sim 10^7$ years and so it is not contemporaneous with the thermal emission from the accretion flow (Punsly 2005). The timescale for the extended emission is so long, it would seem that there must be sources in which the accretion engine has long since shutoff in spite of powerful radio lobe emission 100 kpc away. Where are the "fossil" sources with $Q \sim 5 \times 10^{46}$ergs/s and the accretion flow almost shutoff, $L_{bol} \sim 10^{45}$ergs/s? Perhaps some can be found as distant, $z > 1.5$, 3C narrow line galaxies with improved IR sensitivity. The Spitzer IR telescope is ideal for looking for such hidden kinetically dominated quasars. PKS 1018-42 would be an interesting source for the Spitzer telescope, in order to verify its standing in table 3. However, Spitzer observations to date have not added any new sources to table 3 (Haas et al. 2005). Alternatively, the absence of such sources might tell us something about the fundamental nature of the quasar jet central engine.

REFERENCES

Akujor, C., et al 1991, MNRAS **250** 215

Akujor, C., Garrington, S. 1995, Astron. Astrophys. Suppl. **112** 235

Antonucci, R.J., Ulvestad, J. 1985, ApJ **294** 158

Archibald, E. et al 2001 MNRAS **323** 417

Barthel, P., Tytler, D., Thompson, B. 1990, Astron. and Astrophys. Sup. **82** 339

Bogers, W., Hes, R., Barthel, P., Zensus, J. 1994, Astron. and Astrophys. Sup. **105** 91

Blundell, K., Rawlings, S. 2000, AJ **119** 1111 458

Browne, I.W.A., Perley, R. 1986, MNRAS **222** 149

Elvis, M. et al 1994, ApJS **95** 1

Geldzahler, B.J. & Witzel, A. 1981, AJ, 86, 1306

Gregory, P.C., Vavasour, J.D., Scott, W.K., & Condon, J.J. 1994, ApJS, 90, 173

Haas, M.. et al 2004 A& A **424** 531

Haas, M.. et al 2005 A& A **442L** 39

Hewitt, A. & Burbidge, G. 1993, ApJS, 87, 451

Hintzen, P., Ulvestad, J., Owen, F. 1983, AJ **88** 709.

Hutchings, J., Price, R., Gower, A. 1988 ApJ **329** 122

Laor, A. et al 1997, ApJ **477** 93

Large, M.I., Mills, B.Y., Crawford, D.F. & Sutton, J.M. 1981, MNRAS, 194, 693

Liu, R., Pooley, G., Riley, J. 1992 MNRAS **257** 545

Lonsdale, C., Barthel, P., Miley, G. 1993,ApJS **87** 63

Montovani, F., et al 1992, MNRAS **257** 353

Meisenheimer, K. et al 2001 A& A **372**719

Murphy, D., Browne, I.W.A., Perley, R. 1993, MNRAS **264** 298

Neff, S., Hutchings, J. 1990 AJ **100** 1441

Neff, S., Hutchings, J., Gower, A. 1989 AJ **97** 1291

Punsly, B. 1995, AJ **109** 1555

Punsly, B. 2001, *Black Hole Gravitohydromagnetics* (Springer-Verlag, New York)

Punsly, B. 2005, ApJL **623** L12

Punsly, B., Tingay, S. 2005, ApJL in press

Reid, R. I., Kronberg, P. P., Perley, R. A 1999, ApJS **124** 285

Sault, R.J., Teuben, P.J., Wright, M.C.H. 1995, in ASP Conf. Ser. 77, *Astronomical Data Analysis Software and Systems IV*, ed. R. Shaw, H.E. Payne, J.J.E. Hayes, (San Francisco: ASP), 433

Semenov, V. Dyadechkin, S., Punsly, B. 2004, Science **305** 978

Shepherd, M.C., Pearson, T.J., Taylor, G.B. 1994, BAAS, **26**, 987

Simpson, C. and rawlings, S. 2000 MNRAS **317** 1023

Slee, O. 1995, Aust.J.Phys. **48** 143

Smith, H. E., Spinrad, H. 1980 ApJ **236** 419

Stickel, M., Meisenheimer, K., Kuehr, H. 1994, A&AS**105** 211

Telfer, R., Zheng, W., Kriss, G., Davidsen, A. 2002, ApJ **565** 773

Ulvestad, J., Johnston, K., Perley, R. and Fomalont, E. 1981, AJ, 86, 1010

Veilleux, S. and Bland-Hawthorn, J. 1997, ApJL**476** L105

Veron-Cetty, M.P., Veron, M. 1991, *A Catalogue of Quasars and Active Nuclei* 5th edition, European Southern Observatory Scientific Report No. 10

Veron-Cetty, M.P., Veron, M. 2001, Astron. and Astrophys. **374** 92 **374** 141

Wang, J.-M., Luo, B, Ho, L. 2004, ApJL **615** 9

Willott, C., Rawlings, S., Blundell, K., Lacy, M. 1999, MNRAS**309** 1017

Wright, A.E. et al. 1991, MNRAS, 251, 330

Young, A. et al 2002, ApJ

Zheng, W. et al 1997, ApJ **475** 469

Table 2: The Composite SED of a Radio Quiet Quasar $M_V = -25$

Log ν (Hz) start	Log ν (Hz) end	νF_ν start	νF_ν end	Band	ref
12.5	13.35	44.65	45.3	mid IR	a
13.35	14.4	45.3	44.95	near IR	a
14.4	15.0	44.95	45.45	optical	a,b,c
15.0	15.4	45.45	45.6	UV	b,c
15.4	17.25	45.6	44.3	EUV/soft X-ray	b,c,d
17.25	19.4	44.3	44.3	X-ray	d

[a]Elvis et al. (1994)

[b]Zheng et al. (1997)

[c]Telfer et al. (2002)

[d]Laor et al. (1997)

Table 3: The Most Kinetically Dominated Quasars

Source	z	Q	R	freq	α	ref
		10^{45}ergs/s		$\nu(10^{15}Hz)$		
3C 82	2.878	155.4	10.7	0.014	0.7	a
	2.878	155.4	6.22	1.67	0.7	a
3C 9	2.009	148.3	5.93	1.67	0.36	b
	2.009	148.3	3.82	0.0078	0.36	c
4C 45.21	2.686	59.3	5.11	1.14	-0.12 ± 0.3	b
PKS 1018-42	1.28	65.2	3.38	1.37	1.75	d
	1.28	65.2	4.45	1.07	1.75	d
3C 190	1.195	42.63	13.1	1.34	3.0 ± 0.5	e
	1.195	42.63	1.12	0.133	3.0 ± 0.5	f
	1.195	42.63	2.81	1.07	3.0 ± 0.5	e
TXS 1243+036	3.57	114.8	2.71	0.0016	...	g
3C 405	0.056	23.2	0.75	0.005	...	h
	0.056	23.2	0.93	100	...	i

[a] Semenov et al. (2004)

[b] Barthel et al. (1990) with data recalibrated by M. Vestergaard, private communication

[c] Meisenheimer et al. (2001)

[d] Stickel et al. (1994)

[e] Smith and Spinrad (1980)

[f] Simpson and Rawlings (2000)

[g] Archibald et al. (2001)

[i] Young et al. (2002)